

Investigation of PbO as a system for measuring the electric dipole moment of the electron

D. DeMille,¹ F. Bay,¹ S. Bickman,² D. Kawall,¹ D. Krause, Jr.,² S. E. Maxwell,² and L. R. Hunter²

¹*Department of Physics, P.O. Box 208120, Yale University, New Haven, Connecticut 06520*

²*Department of Physics, Amherst College, Amherst, Massachusetts 01002*

(Received 22 September 1999; revised manuscript received 6 January 2000; published 10 April 2000)

We point out the potential of the diatomic molecule PbO as a system in which to search for an electron electric dipole moment (EDM). Large oscillator strengths between various electronic states of PbO would be beneficial for such an experiment. As a step toward determining these oscillator strengths, we have measured a number of radiative lifetimes and branching ratios in PbO. We discuss the impact of our measurements on the proposed EDM experiment and point out the need for further experimental and theoretical work on PbO.

PACS number(s): 33.70.Ca, 33.90.+h, 14.60.Cd, 13.40.Em

I. INTRODUCTION

The electric dipole moment of the electron (d_e) is of great interest in particle physics [1,2]. According to the standard model, d_e is too small to be detected by any presently conceivable method. However, many currently favored extensions to the standard model (in particular, supersymmetric models) predict $|d_e|$ to be within ~ 3 orders of magnitude of the current experimental limit: $|d_e| < 4 \times 10^{-27}$ e cm [3]. An increase of sensitivity by several orders of magnitude would make it possible to either exclude a wide variety of these theoretical models or to see evidence of new physics beyond the standard model.

We plan to search for the electric dipole moment (EDM) of the electron by using the metastable excited state $a(1)[^3\Sigma^+]$ of the diatomic molecule PbO [4]. (For clarity, we will refer to this state in the text as “ $a(1)$ ” rather than simply “ a .”) The proposed experiment ultimately could be sensitive to an electron EDM $|d_e| < 10^{-31}$ e cm, i.e., ~ 4 orders of magnitude below the current limit. This sensitivity arises from a unique combination of properties of PbO, which simultaneously provide a large enhancement factor, narrow magnetic resonance lines, and high counting rates.

In this paper, we begin by outlining the proposed EDM experiment using PbO. This discussion will explain the importance of measuring various parameters of electronic transitions in PbO. In the second part of the paper, we describe our experimental investigation of some of these parameters. Finally, we discuss the implications of our results for the eventual EDM measurement.

II. THE PROPOSED EDM EXPERIMENT IN PbO

A. General features of EDM experiments

The signature of an EDM is a linear, Stark-induced energy shift $\Delta E = -d\hat{J} \cdot \vec{\mathcal{E}}$, where $\hat{J} = \vec{J}/|J|$ is a unit vector along the angular momentum of the system, $\vec{\mathcal{E}}$ is the electric field experienced by the system, and d is the value of the permanent electric dipole moment. The ultimate sensitivity of any experiment searching for an EDM depends on both the size of the energy shift $\Delta E = |d\mathcal{E}|$ and the ability to accurately measure this small quantity. The design of an EDM experiment usually involves tradeoffs between the optimization of the factors that determine the attainable statistical

sensitivity. For example, the size of ΔE depends on the choice of experimental system (e.g., atoms vs molecules) and also on technical parameters such as the maximum external electric field that can be applied without breakdown. At the same time, good energy resolution demands long coherence times (τ) and high counting rates (dN/dt), since the optimum energy resolution (determined by the limitations of shot noise) is $\delta(\Delta E) = \hbar/[\tau\sqrt{T(dN/dt)}]$, where T is the total observation time.

B. Enhancement factor and effective electric field

Here we are concerned specifically with the electron EDM. For good sensitivity to d_e , it is of course optimal to use a system with one or more unpaired electron spins (since otherwise the EDMs will cancel in pairs). For such a paramagnetic system, the linear Stark shift can be written as $\Delta E = -d_e \mathcal{E}_{\text{eff}}$, where \mathcal{E}_{eff} is the effective electric field experienced by a valence electron. From rotational symmetry it is easily seen that $\mathcal{E}_{\text{eff}} = 0$, unless an external electric field $\vec{\mathcal{E}}_{\text{ext}}$ is applied to the system. Even in the presence of $\vec{\mathcal{E}}_{\text{ext}}$, the effective field is nonzero only because of relativistic effects [5]. It has long been known that, nevertheless, $|\mathcal{E}_{\text{eff}}|$ can exceed $|\mathcal{E}_{\text{ext}}|$ by many orders of magnitude for suitably chosen systems [6].

The fact that the effective electric field can be larger than the external electric field is usually expressed in terms of an “enhancement factor” $R \equiv \mathcal{E}_{\text{eff}}/\mathcal{E}_{\text{ext}}$. However, this language is inadequate for describing the relationship between external and effective fields in a molecule. More generally, the effective electric field experienced by the valence electron(s) in an atom or molecule can be expressed in the form $\mathcal{E}_{\text{eff}} = Q\mathcal{P}$, where Q is a factor which includes both the relativistic effects and details of atomic/molecular structure, and \mathcal{P} is the degree of polarization of the system by the external field [7]. For both atoms and molecules, typical values are $Q \sim (10-100) \times 10^9$ V/cm $\times (Z/80)^3$; here the Z dependence reflects both the relativistic nature of the effective field and the size of the internal electric field near a heavy nucleus [6,8]. In the ground state of atomic Cs ($Z=55$), for instance, $\mathcal{E}_{\text{eff}} \sim (6 \times 10^9$ V/cm) \mathcal{P} . For comparison, it has been calculated that in the $a(1)$ state of PbO, $\mathcal{E}_{\text{eff}} = (6 \times 10^9$ V/cm) \mathcal{P} [9].

C. Using molecules to search for the electron EDM

There is a qualitative difference between the laboratory values of effective fields in atoms and molecules, because the values of \mathcal{P} that can be achieved are very different for these systems [7]. For atoms, \mathcal{P} is limited by the size of the electric fields achievable in the laboratory; for typical atomic ground states, $\mathcal{P}_{\text{atom}} \sim 10^{-3} [\mathcal{E}_{\text{ext}}/(100 \text{ kV/cm})]$. (This fact explains the language of the ‘‘enhancement factor’’ used to describe the effective field in atoms; in this regime of $\mathcal{P} \ll 1$, $\mathcal{P} \propto \mathcal{E}_{\text{ext}}$ and the ratio $R \equiv \mathcal{E}_{\text{eff}}/\mathcal{E}_{\text{ext}}$ is a constant.) In contrast, with polar molecules $\mathcal{P} \approx 1$ can be achieved with modest external fields. Thus the observable energy shifts, caused by an electron EDM, can be 100–1000 times greater for heavy, polar, paramagnetic molecules than for atoms. For a concrete comparison, we note that the experiment which gives the best limit on d_e uses atomic Tl ($R \sim -600$) and an external electric field $\mathcal{E}_{\text{ext}} \sim 100 \text{ kV/cm}$ to achieve an effective field $|\mathcal{E}_{\text{eff}}| \sim 6 \times 10^7 \text{ V/cm}$ [3]; the effective field for fully polarized PbO in the $a(1)$ state will be ~ 100 times larger than this.

Until now, however, it has seemed that the increased size of the effect ΔE , which can be achieved by using molecules, would be offset by enormous losses in energy resolution $\delta(\Delta E)$. For two reasons the use of molecules has seemed to imply dramatically reduced counting rates (and thus poorer resolution), compared to experiments using atoms. First, heavy molecules that are paramagnetic in their ground states (e.g., HgF and YbF) are chemical radicals, which usually require extreme thermal and chemical conditions for production [10]; this in turn has meant relatively low production rates for the desired species. Second, the Boltzmann distribution spreads the molecular population over many rotational sublevels ($\sim 10^4$ under typical conditions $T \gtrsim 1000 \text{ K}$), while only one of the lowest levels is useful for an EDM experiment (which requires states of well-defined energy and angular momentum). Until now, the only technologically feasible means of radical production that has seemed compatible with the many requirements of an EDM experiment has been in the relatively low-density environment of a molecular beam [7].

D. The rationale for using PbO to search for the electron EDM

The particular attractiveness of using the $a(1)$ state of PbO arises from the possibility of attaining much higher counting rates than had seemed possible with molecules. These higher counting rates can be obtained by working in a vapor cell rather than a molecular beam: a cell can have much larger volume and density of molecules than is possible in a beam. (These advantages of working in a vapor cell are exploited in several ongoing atomic EDM experiments [11,12].) However, the ability to work in a vapor cell is, we believe, entirely novel for *molecular* EDM experiments, and is possible only because several conditions can be simultaneously met with PbO.

First, PbO (in its diamagnetic $X(0)[^1\Sigma^+]$ ground state) is thermodynamically and chemically stable; it can be routinely obtained and easily vaporized. In order to attain good sensitivity to the electron EDM, the paramagnetic $a(1)$ state must

be populated; this can be accomplished by selective and efficient laser excitation. Thus working in this metastable state of PbO circumvents the thermochemical extremes previously considered necessary for using paramagnetic molecules.

Second, the $a(1)$ state of PbO requires only small electric fields, $\mathcal{E} \gtrsim 10 \text{ V/cm}$, to achieve $\mathcal{P} \approx 1$. Such modest fields have been achieved routinely in heated cells [13], but much larger fields are difficult to apply without discharges in the hot, dense vapor of a closed cell. The extremely high polarizability of the $a(1)$ state is a consequence of the very small energy splitting of $\sim 12 \text{ MHz}$ between the Ω -doublet opposite parity levels in this state [14]. Such small splittings are a systematic feature of Hund’s case (c) states with $|\Omega| \gtrsim 1$ [15]. In contrast, true molecular radicals (i.e., molecules which are paramagnetic in their ground states such as YbF and HgF) typically have $|\Omega| = \frac{1}{2}$ ground states, for which $\mathcal{E} \gtrsim 10 \text{ kV/cm}$ is required to achieve $\mathcal{P} \approx 1$ [7].

E. Estimate of statistical sensitivity in a PbO EDM experiment

Now we consider the statistical sensitivity to the electron EDM, which can be achieved using a vapor cell of PbO. An optimum experiment would maximize the coherence time (τ) and the counting rate (dN/dt). The coherence time for measurements in the $a(1)$ state can be no larger than the lifetime $\tau_a \sim 80 \mu\text{s}$ [16]. To avoid even shorter values of τ , it is necessary to prevent molecular collisions from destroying the orientation or alignment of the $a(1)$ state; thus we demand $\tau_{\text{collision}} > \tau_a$. This leads to a constraint on the useful vapor density (n) of PbO. With a conservative estimate of the relaxation cross section ($\sigma_{\text{collision}} \sim 10^{-14} \text{ cm}^2$), the total density can be as large as $n \sim 3 \times 10^{13} \text{ cm}^{-3}$. This density corresponds to the saturated vapor pressure $P \sim 3 \times 10^{-3} \text{ Torr}$, attained at a temperature of $\sim 690 \text{ }^\circ\text{C}$ [17]. It is also necessary to avoid decoherence of the $a(1)$ state due to wall collisions. This can be avoided by choosing cell dimensions (L) such that $\tau_{\text{wall}} = L/v > \tau_a$, where v is the rms thermal velocity. Demanding $L \sim 2\tau_a v$ leads to reasonable dimensions $L \sim 5 \text{ cm}$.

At the temperature corresponding to maximum PbO density, the fraction of molecules (f) in the lowest rotational level is $f \sim B/kT \sim 3 \times 10^{-4}$, where $B = 4 \times 10^{-5} \text{ eV}$ is the rotational energy constant [18]. Assuming a roughly cubic cell volume, the number of molecules in the lowest rotational level (N_0) is then $N_0 \sim fnL^3 \sim 10^{12}$. If these molecules are excited to and detected from the $a(1)$ state with total efficiencies ε_e and ε_d , respectively, the counting rate will be $dN/dt = \varepsilon_e \varepsilon_d N_0 / \tau_a \sim \varepsilon_e \varepsilon_d 10^{16}/\text{s}$.

We can now determine the statistical sensitivity to the electron EDM for an experiment using PbO. We recall the following data from the preceding discussion: the energy shift $|\Delta E| = d_e \mathcal{E}_{\text{eff}}$, where $\mathcal{E}_{\text{eff}} \sim 6 \times 10^9 \text{ V/cm}$, and the energy resolution $\delta(\Delta E) = \hbar / [\tau \sqrt{T(dN/dt)}]$, where $\tau \sim 80 \mu\text{s}$ and $dN/dt \sim \varepsilon_e \varepsilon_d 10^{16}/\text{s}$. Combining these factors, we find that if $\varepsilon_e \varepsilon_d \sim 1$, $T = 1$ day of integration would give a statistical sensitivity $\delta(d_e) < 10^{-31} \text{ e cm}$, which corresponds to an improvement of more than 10^4 on the current limit for d_e [3].

F. Efficiencies and sensitivity in a simple version of the PbO EDM experiment

Next we discuss whether it is indeed possible to achieve such good efficiency of both excitation and detection of the $a(1)$ state of PbO. Let us consider first a conceptually simple design of the PbO experiment in order to demonstrate some of the issues involved in answering this question. In this simple version of the experiment, we imagine populating the $a(1)$ state by direct excitation of the $X \rightarrow a$ transition, and detecting the $a(1)$ state by observing the fluorescence accompanying its decay. (More specifically, the orientation or alignment of the $a(1)$ state can be detected by observing quantum beats in the fluorescence [19].)

It should come as no surprise that it is difficult to efficiently populate the $a(1)$ state. The long lifetime of this state necessarily means that the X - a oscillator strength is small, and thus that high laser power is required to populate the $a(1)$ state via the X - a transition. (Note also that the choice of such a long-lived state is not arbitrary; rather, the requirement for good energy resolution in the EDM experiment makes the use of such a state necessary). In order to quantify this statement, we note that $\varepsilon_e = 1$ means that PbO ground-state molecules from the entire velocity distribution and the entire volume of the cell must be transferred to the $a(1)$ state, once per lifetime τ_a . If we define a cross section for laser excitation σ_e (averaged over the velocity distribution in the cell), then for a given average laser flux over the cell (F), the average excitation rate (R) is $R \sim F\sigma_e$, and the excitation efficiency is $\varepsilon_e \sim R\tau_a$.

The cross section can be estimated from the standard formula [20] $\sigma_e = (\lambda^2/8\pi)(\Gamma_{\text{partial}}/\Gamma_{\text{Doppler}})$, where $\lambda \sim 560$ nm is the wavelength of the laser light, Γ_{partial} is the decay rate of $a(1)$ into a specific rovibrational level of X , and $\Gamma_{\text{Doppler}} \sim 2\pi \times 800$ MHz is the Doppler width. With our knowledge of τ_a , and with reasonable estimates of branching ratios into various rovibrational levels, we find $\sigma_e \sim 3 \times 10^{-17}$ cm². This in turn means that achieving $\varepsilon_e = 1$ in the direct excitation $X \rightarrow a$ would require a time-averaged laser power of ~ 1000 W incident on the cell. This value is probably unattainable. With a standard commercial dye laser providing a few watts of average power, only $\varepsilon_e \sim 3 \times 10^{-3}$ can be attained.

The detection efficiency will be similarly poor in this simple experimental arrangement. Detection of the decay fluorescence from the $a(1)$ state is inefficient for a variety of reasons. First, it is difficult to collect light over a large solid angle (Ω) surrounding a heated vapor cell; we estimate that $\Omega \sim 0.1$ is the largest feasible value. Suppressing backgrounds from blackbody radiation and scattered laser light requires the use of bandpass filters which transmit fluorescence accompanying decay to only a single vibrational level of X . Taking into account branching ratios, filter transmission, and detector quantum efficiency, we expect a total detection efficiency of only $\varepsilon_d \sim 5 \times 10^{-3}$.

Note that even this simple experimental arrangement has sufficient sensitivity to place interesting limits on d_e . With a reasonable integration time of ~ 1 week, the statistical uncertainty can reach $\delta(d_e) < 10^{-29}$ e cm, already a factor of 100 below the current limit. In addition, the Ω -doublet level

structure of PbO leads to a number of unique and powerful means for rejecting systematic effects. (Discussion of systematics in the EDM experiment is beyond the scope of this paper, but will be addressed in a subsequent publication [21].) Thus we believe that a sensitivity to $|d_e|$ at the level 10^{-29} e cm is feasible with the simple configuration described here; such an experiment is now under way. Nevertheless, it would be of great interest to find methods to increase the excitation and/or detection efficiencies by significant factors, and thus to potentially improve the sensitivity to $|d_e|$ by up to another factor of ~ 100 .

G. Toward improved efficiency of the PbO EDM experiment

It seems likely that higher efficiency can be achieved in both the excitation and detection of the $a(1)$ state by using a slightly more complex experimental configuration. As we explain here, the key to improved efficiencies is the existence of strong electronic transitions of the form $a \leftrightarrow Y$, where we use Y as a generic label for any of several excited electronic states of PbO. There has been no experimental data on such transitions; filling this gap is the motivation for much of the experimental work described later in this paper.

We consider first the implications of such $a \leftrightarrow Y$ transitions in the efficiency for excitation of the $a(1)$ state. It seems likely that ε_e can be improved by exciting the $a(1)$ state via a two-photon, stimulated Raman process of the type $X \rightarrow Y \rightarrow a$. We argue that both steps of this process can probably be accomplished with greater efficiency than the direct $X \rightarrow a$ process, given the limitations of available laser sources.

There are a number of excited states Y of PbO which [unlike the $a(1)$ state] have been observed in absorption from the ground state X [22]. Therefore it is known that the transitions $X \rightarrow Y$ for these states ($Y = A, B, C, C', D, E, F,$ and G) are much stronger than direct $X \rightarrow a$ transitions (although in many cases there is no quantitative measure of the $X \rightarrow Y$ oscillator strengths). Thus for any of these states the step $X \rightarrow Y$ can be saturated with far less laser power than the 1 kW required for direct $X \rightarrow a$ excitation.

The strength of the transitions $Y \rightarrow a$ also can be expected to be greater than that of the direct $X \rightarrow a$ transition. The $X(0)[^1\Sigma^+] \rightarrow a(1)[^3\Sigma^+]$ transition is forbidden by the selection rule $\Delta S = 0$, and in addition the spatial part of the dipole matrix element appears to be suppressed. Thus the $X \rightarrow a$ transition is considerably weaker even than other nominally forbidden ($\Delta S \neq 0$) transitions in PbO such as $X \rightarrow A, B, C, C'$ [23]. In contrast to the situation for $X \rightarrow a$, there are no selection rules to forbid many of the transitions $Y \rightarrow a$. Therefore, it can be broadly expected that at least some of these $Y \leftrightarrow a$ oscillator strengths are appreciable. In order to determine the best scheme for high-efficiency excitation of the $a(1)$ state via a two-step process $X \rightarrow Y \rightarrow a$, it will be necessary to identify strong $Y \rightarrow a$ transitions and, further, to measure the oscillator strengths for both the $X \rightarrow Y$ and $Y \rightarrow a$ steps of the Raman transitions.

Next consider the requirements for efficient detection of the $a(1)$ state. An improved value of ε_d can be achieved using laser absorption, if the cell comprises ~ 1 absorption

length for the probe laser (see, e.g., Ref. [1]). Based on our estimates of the available column density nL of PbO in the $a(1)$ state, this condition can be met for a transition of the form $a \rightarrow Y$ if the oscillator strength for that transition is ~ 1 . From the usual sum-rule condition for oscillator strengths (see, e.g., Ref. [20]), it is reasonable to expect that such a transition exists. Unlike for the pump transition, we note that the upper state Y of the probe transition need not have any appreciable coupling to the ground state X . However, no states of PbO without such coupling have been observed. Finally, we point out that the conditions imposed on the strength of both the population and probe transitions could be relaxed somewhat by arranging for multiple passes of the laser beam through the vapor cell; however, this is a technically difficult problem in itself.

Here we report the first steps toward learning to take full advantage of the PbO system for a measurement of the electron EDM. We have measured lifetimes for most known excited states of PbO (a , A , B , C , C' , and D). In addition, we have searched for appreciable coupling of the higher-lying states to the $a(1)$ state: excitation of $X \rightarrow Y$ transitions, followed by selective observation of $Y \rightarrow X$ and $a \rightarrow X$ fluorescence intensities, has yielded $(Y \rightarrow X)/(Y \rightarrow a)$ branching ratios. In combination with known energies and estimated Franck-Condon factors, we have deduced from our data some approximate values for $X \rightarrow Y$ and $a \rightarrow Y$ transition matrix elements. Following the description of the experiment, we will discuss the implications of our results for the EDM search using PbO.

III. EXPERIMENTAL INVESTIGATION OF ELECTRONIC TRANSITIONS IN PbO

A. General description of the apparatus

Our investigations are performed using a conventional effusive molecular-beam apparatus. PbO is heated in a stainless-steel oven to a temperature of about 900 K. Apertures in the heat shields collimate the PbO beam. The PbO is selectively excited with light generated by a Nd:YAG pumped dye laser with frequency-doubling capabilities. The frequency resolution of the apparatus is limited in the visible range to about 0.2 cm^{-1} by the laser linewidth. This linewidth is typically sufficient to resolve individual rotational levels, except near bandheads. The decay fluorescence is collimated by a collection lens, passes through a pair of interference filters (typically with a bandpass of 10 nm) to select the frequency, and is focused onto a photon-counting photomultiplier tube with known quantum efficiency. The interference filters are narrow enough that they typically select a single vibronic decay channel. The photon counts are recorded by a gated photon counter (Stanford Research SR400) or a multichannel scaler (Stanford Research SR430).

B. Lifetime measurements

Lifetime measurements are made by counting the number of fluorescence photons as a function of the delay from the initial laser pulse. The signals are recorded using either multiple measurements with variable delays on the photon

TABLE I. Measured lifetimes in PbO. Reference (a) is Ref. [12]. Ref. (b) is Ref. [7]. The fifth vibrational level of C' is unmeasured because the bandhead was unresolved from lines associated with the seventh vibrational level of C .

Electronic state	Vibrational level	Lifetime (μs)	
		Present work	Other experiments
A	2		3.74(30) (a)
A	3	3.68 (6)	
B	0, 1		2.58(30) (a)
B	2	3.03(12)	
C	4	2.96(14)	
C	7	2.83(7)	
C'	3	3.7(2)	
C'	4	3.9(2)	
C'	6	3.4(2)	
D	1	0.368(10)	
a	2	101(10)	
a	3	110(7)	81.8(5.5) (b)
a	4	78(6)	
a	5	77(5)	
a	6	87(11)	

counter or, in later measurements, with the multichannel scaler. Data are collected both on the rotational bandhead and off resonance (detuned typically $1\text{--}2 \text{ cm}^{-1}$ to the blue of the red-shaded bandhead). Taking the difference between these data eliminates backgrounds associated with scattered light, window fluorescence, dark noise, and blackbody radiation. Several independent measurements of the lifetime are made with the excitation laser at different positions and powers. No systematic dependence on laser power is observed, suggesting that saturation of our detection system is not an issue. The data collected at different laser positions permit us to place reasonable bounds on possible contributions to the measured lifetime due to spatial variations of the detection efficiency. Because the short and long lifetimes require different techniques, they will be discussed separately, beginning with the shorter-lived states.

The A , B , C , C' , and D lifetimes are extracted simply by evaluating a best-fit exponential decay to the data. Data from times just after the laser pulse (typically $\sim 100 \text{ ns}$) are excluded from the fit, because of backgrounds from scattered laser light, laser-induced fluorescence from windows, etc. Data are collected with the laser intersecting the atomic beam at the center of the viewing region, and at positions 3 mm upstream and downstream from center. The statistical uncertainty associated with each of these individual measurements is typically only $1\text{--}2\%$. The larger uncertainties quoted in Table I accommodate the ranges of lifetimes measured at the various positions of the laser beam. The results obtained for the A and B states are in reasonable agreement with earlier, less precise measurements [23]. We are not aware of any previous measurements of the C , C' , and D lifetimes.

Measurements of the $a(1)$ state are more problematic due to its long lifetime. Typically, the molecules traverse the

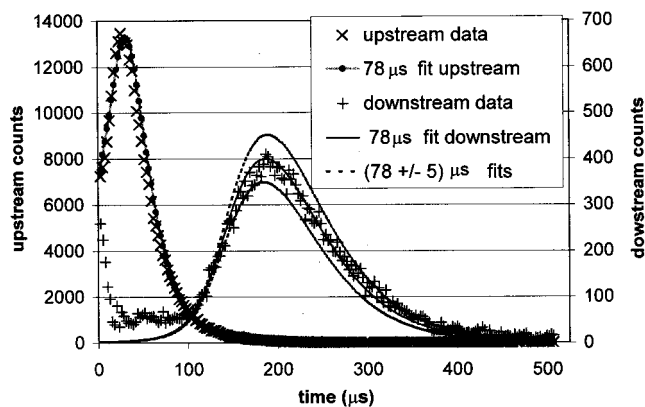


FIG. 1. Typical data and fits used to determine the $a(1)$ state lifetime. The data shown are for the $v'=5$ state. The solid curves are the best fits to the data; the dotted curves show the fits with the lifetime changed by $\pm 5 \mu\text{s}$, which is the range of uncertainty assigned for this data set.

viewing region within a few tens of microseconds, making the measurement of the lifetime difficult. To solve this problem we measure the decay fluorescence in two viewing regions separated by three inches. The laser beam now intersects the atomic beam 12–14 mm upstream from the center of the “upstream” viewing region. Two independent detector assemblies are used. One detector constantly monitors the total decay fluorescence in the upstream region for normalization. On the opposite side of the atomic beam, a second detector assembly is moved back and forth between the “upstream” and “downstream” detection regions. The two interaction regions have been made as identical as possible and methods have been developed to allow precise positioning of the detector assembly. Care is taken that all of the parameters of the detection apparatus are left unchanged when the detector assembly is moved between the two regions. The signals and backgrounds in each of these regions are recorded on the multichannel scaler. All signals are normalized using the signal from the fixed detector, effectively removing variations in signal size that might occur between measurements (due to, e.g., fluctuations in the laser or the atomic beam). The measured fluorescence data are fit to a numerical simulation that predicts the expected fluorescence as a function of time in the two regions. The collection efficiency as a function of the position of the radiating molecules is determined by an auxiliary measurement, and the resulting profile is used in the numerical simulation. The fit parameters adjusted in the simulation are the overall amplitude, the effective beam temperature, the position of the point of laser excitation, and the lifetime. A typical fit is shown in Fig. 1. Statistical uncertainties in the fit lifetimes are very small (typically less than 1%). The inferred lifetime depends primarily on the relative heights of the peaks in the two regions and changes by less than 2% when the effective beam temperature used in the fit is varied by 100 C from its best-fit value. The combined uncertainties in the $a(1)$ lifetimes quoted in Table I are dominated by the uncertainties in the detection efficiency as a function of position. In particular, reflections of the primary fluorescence from the vacuum

chamber are not taken into account in the simulation. We believe that these reflections account for the discrepancy between our fit and the data in the downstream region at short times (see Fig. 1). For this reason, we have restricted the fit in the downstream region to data taken at times greater than $120 \mu\text{s}$. Similarly, to avoid overweighting data that contain little signal, data where the background is large compared to the signal are also ignored (this is typically data taken at times greater than $100 \mu\text{s}$ in the upstream and $300 \mu\text{s}$ in the downstream region).

Our measured $a(1)$ lifetime on the $v'=3$ vibrational bandhead is somewhat longer than that obtained in Ref. [16]. This is perhaps not too surprising, since the earlier measurement took the decay rates measured in the presence of buffer gas, and extrapolated to zero pressure. It is interesting to note that the lifetimes of the $v'=2$ and 3 levels are significantly longer than the higher vibrational levels, consistent with the suggestion of Beattie *et al.* [16].

C. Branching ratios

One of the prime motivations for the present work is to determine if there are strong transitions that couple other excited molecular levels to the $a(1)$ state, since such transitions could be used to improve the excitation and/or detection of the $a(1)$ state. We have searched for such a coupling from the $Y=A, B, C, C'$, and D levels. To search for a branch from $Y \rightarrow a$, two detection systems observe the interaction volume from opposite sides of the atomic beam. One of these has filters that permit us to monitor a specific vibronic channel of the decay $Y \rightarrow X$. The second system is set to monitor a likely vibronic transition in the subsequent cascade decay $a \rightarrow X$. The second channel accepts signals only after a delay of $10 \mu\text{s}$ after the laser pulse, in order to further distinguish decays proceeding through the long-lived $a(1)$ state from the direct decays of the upper state Y . The likely decay paths are chosen by using Franck-Condon (FC) factors. For $Y=A$ and B we use FC factors published by Dorko *et al.* [24], while for $Y=C, C'$ and D we generate FC factors from a Morse potential that is generally found to yield good agreement with the published values for other transitions, and with qualitative measures of relative absorption intensities [22].

To measure the branch, we record the signals in both channels as we scan the laser over some high rotational states. This produces a large, modulated signal that allows for sensitive detection of the branch. We search for correlation between the signals in the two detection channels. The results of our search for all of the states are summarized in Table II. For $Y=A, B, C$, and D we are not able to definitively measure a nonzero branch. However, for several vibrational levels of C' we do see clear evidence for $C' \rightarrow a$ transitions. Typically, we find that the ratio of the detected photons, $R \equiv (C' \rightarrow a \rightarrow X)/(C' \rightarrow X)$, is several percent. Unfortunately, given our distrust of the FC factors from our measurements of $X \rightarrow a \rightarrow X$ (see below), it is difficult to make precise statements about the transition strengths at this point.

TABLE II. Branching ratios for known levels to decay via the $a(1)$ state vs decaying directly to the ground state X . A single vibronic level was excited, and the detection was sensitive only to specific vibronic decays. The level with vibrational number ν of electronic state Y is denoted as $Y[\nu]$. Column 1 lists the channels monitored; the transition in curly brackets specifically is detected. Column 2 lists the wavelengths of the detected fluorescence for each channel. Column 3 lists the ratio of photons emitted in the two monitored channels, taking into account different detection efficiencies for the two channels. Column 4 lists the transitions and the associated wavelengths which would be required for populating the $a(1)$ state via a stimulated Raman transition. Unambiguous branching to the $a(1)$ state is observed only from the C' state. The listed uncertainties only reflect the deviation of the branching ratio from zero; there is an additional uncertainty of $\pm 40\%$ in the relative detection efficiencies for the two fluorescence channels.

Decay channels (channels monitored)	Wavelengths detected	Ratio of photon yields	Transition for stimulated Raman excitation (associated wavelength)	
$A[1] \rightarrow \{a[1] \rightarrow X[2]\}$ $\{A[1] \rightarrow X[2]\}$	$\{668 \text{ nm}\}$ $\{533 \text{ nm}\}$	$1.6(7.8) \times 10^{-2}$	$X[0] \rightarrow A[1]$ (496 nm)	$A[1] \rightarrow a[1]$ (2641 nm)
$A[3] \rightarrow \{a[3] \rightarrow X[0]\}$ $\{a[3] \rightarrow X[3]\}$	$\{577 \text{ nm}\}$ $\{528 \text{ nm}\}$	$1.7(0.6) \times 10^{-2}$	$X[0] \rightarrow A[3]$ (475 nm)	$A[3] \rightarrow a[3]$ (2678 nm)
$B[2] \rightarrow \{a[3] \rightarrow X[0]\}$ $\{B[2] \rightarrow X[7]\}$	$\{577 \text{ nm}\}$ $\{546 \text{ nm}\}$	$2.6(1.0) \times 10^{-3}$	$X[0] \rightarrow B[2]$ (432 nm)	$B[2] \rightarrow a[3]$ (1714 nm)
$C[4] \rightarrow \{a[4] \rightarrow X[0]\}$ $\{C[4] \rightarrow X[3]\}$	$\{562 \text{ nm}\}$ $\{426 \text{ nm}\}$	$2.5(1.8) \times 10^{-2}$	$X[0] \rightarrow C[4]$ (388 nm)	$C[4] \rightarrow a[4]$ (1246 nm)
$C'[3] \rightarrow \{a[3] \rightarrow X[0]\}$ $\{C'[3] \rightarrow X[5]\}$	$\{577 \text{ nm}\}$ $\{439 \text{ nm}\}$	$7.8(1.9) \times 10^{-2}$	$X[0] \rightarrow C'[3]$ (380 nm)	$C'[3] \rightarrow a[3]$ (1115 nm)
$C'[3] \rightarrow \{a[3] \rightarrow X[0]\}$ $\{C'[3] \rightarrow X[4]\}$	$\{577 \text{ nm}\}$ $\{426 \text{ nm}\}$	$7.0(3.7) \times 10^{-2}$		
$C'[4] \rightarrow \{a[4] \rightarrow X[0]\}$ $\{C'[4] \rightarrow X[4]\}$	$\{562 \text{ nm}\}$ $\{418 \text{ nm}\}$	$4.9(1.2) \times 10^{-2}$	$X[0] \rightarrow C'[4]$ (374 nm)	$C'[4] \rightarrow a[4]$ (1113 nm)
$C'[6] \rightarrow \{a[6] \rightarrow X[0]\}$ $\{C'[6] \rightarrow X[5]\}$	$\{535 \text{ nm}\}$ $\{413 \text{ nm}\}$	$2.5(0.4) \times 10^{-2}$	$X[0] \rightarrow C'[6]$ (361 nm)	$C'[6] \rightarrow a[6]$ (1111 nm)
$D[1] \rightarrow \{a[3] \rightarrow X[0]\}$ $\{D[1] \rightarrow X[3]\}$	$\{577 \text{ nm}\}$ $\{351 \text{ nm}\}$	$2(3) \times 10^{-4}$	$X[0] \rightarrow D[1]$ (327 nm)	$D[1] \rightarrow a[3]$ (753 nm)

D. Other observations

The E state

Despite many attempts, we were unable to observe the E state in fluorescence. This is puzzling since the X - E transition has been seen both in absorption [22] and in fluorescence [24]. It is possible that the lifetime of E is simply shorter than the recovery time of our detection system from the large pulse of scattered light and UV-induced fluorescence during and following the laser pulse. This would require $\tau(E) < 100$ ns. However, we cannot rule out that the E state is ionized or dissociated by the excitation laser before it has a chance to decay radiatively.

X - a Franck-Condon factors

In the course of measuring the $a(1)$ state lifetime for various vibrational levels, we have been able to determine roughly the relative transition strengths for different excitation-detection chains of the form $X(\nu'') \rightarrow a(\nu') \rightarrow X(\nu''^*)$. This allows us to determine relative values of products of FC factors for the X - a transition (see Table III). Also shown in the table are the predictions for these values

from the previously calculated FC factors [24]. The experimental values of these parameters could be in error by as much a factor of 2 due to variations in various parameters from run to run. Despite these large uncertainties, it is apparent that the calculated FC factors are woefully inadequate to describe the observations.

IV. CONCLUSIONS

Now we consider the implications of our measurements for the PbO EDM experiment discussed in Sec. II. We first note that the single transition of the type $a \rightarrow Y$ that we have observed—the $a \rightarrow C'$ transition—is probably not sufficiently strong to enable efficient detection by absorption. We estimate that a PbO cell of the type described in the introduction would comprise only $\sim 10^{-3}$ absorption lengths for this transition. On the other hand, both this transition and the $X \rightarrow C'$ transition are considerably stronger than the direct $X \rightarrow a$ transition. For this reason, it should be possible to enhance the population of the $a(1)$ state by driving the $X \rightarrow C' \rightarrow a$ process rather than the direct excitation $X \rightarrow a$. Accurate calculations of the relative efficiency of these pro-

TABLE III. A comparison of the theoretical and observed products of the Franck-Condon factors $\{F(v'',v') \times F(v'',v')\}$ for transitions from $X[v''] \rightarrow a[v'] \rightarrow X[v''^*]$. The calculated values are taken from Ref. [13]. To facilitate comparison, both observed and calculated values have been normalized to their respective values for the $X[1] \rightarrow a[3] \rightarrow X[0]$ transition. Uncertainties in the observed values are $\sim 50\%$.

States involved in the transitions			$\frac{F(v'',v') \times F(v'',v')}{F(1,3) \times F(0,3)}$	$\frac{F(v'',v') \times F(v'',v')}{F(1,3) \times F(0,3)}$
v'' initial of X	v' of a	v''^* final of X	Calculated	Observed
1	2	0	0.7	0.4
1	3	0	1.0	1.0
1	4	0	0.7	2.4
1	5	0	0.2	2.6
1	6	0	<0.1	0.6
2	2	0	0.5	0.5
2	3	0	0.1	0.8
1	1	2	1.2	<0.1

cesses are not possible because we lack reliable FC factors for all steps. However, our best estimate indicates that an enhancement of the excitation rate by a factor of ~ 10 can be achieved using optimized laser sources.

It is our hope that this study will initiate new theoretical work on the structure of PbO, which may provide answers to some of the questions raised by our observations. In particular, four features of our data are difficult to explain from our current knowledge of the PbO structure. (i) Why does the $a(1)$ state couple fairly strongly only to C' , and not to any of the other nominal triplet states? (ii) Why does the lifetime of the $a(1)$ state vary as a function of vibrational quantum number? (iii) Why are the calculated FC factors for the X - a transition inadequate to explain the observed transition rates? (iv) Why were we unable to observe emission signals for the $X \rightarrow E$ transition?

We intend to continue our spectroscopic investigations of PbO. Although our tentative result for the $X \rightarrow C' \rightarrow a$ cross section is encouraging, we will continue to investigate excited states of PbO in an effort both to measure the relevant FC factors and to locate previously unobserved states

that couple more strongly to the $a(1)$ state. These measurements will be conducted in a vapor cell in order to achieve larger signals. We are also beginning a project to perform high-resolution molecular beam measurements on the $a(1)$ state. Precise values of the hyperfine structure, isotope shift, and Lande g factors for this state will permit a more precise semiempirical calculation of the sensitivity of the proposed EDM experiment to d_e [25].

ACKNOWLEDGMENTS

We wish to thank D. Budker for originally pointing out to us the possible application of PbO to an EDM measurement, and for many subsequent helpful discussions. We also thank P. Grant for technical assistance and M. Kozlov and R. Field for useful conversations. This work was supported by funds from Amherst College, Yale University, Research Corporation, and the National Science Foundation under Grant No. 9402701NSF.

- [1] A recent review of the motivations for and techniques used in all EDM experiments is I. B. Khriplovich and S. K. Lamoreaux, *CP Violation Without Strangeness: Electric Dipole Moments of Particles, Atoms, and Molecules* (Springer, New York, 1997).
- [2] Reviews of the predictions for d_e in various models are given in M. Suzuki, *Rev. Mod. Phys.* **63**, 313 (1991); S. Barr, *Int. J. Mod. Phys. A* **8**, 209 (1993).
- [3] E. Commins, S. Ross, D. DeMille, and B. Regan, *Phys. Rev. A* **50**, 2960 (1994).
- [4] This was first suggested in V. Flambaum, Ph.D. thesis, Institute of Nuclear Physics, 1987; see also L. Barkov, M. Zolotarev, and D. Melik-Pashaev, *Kvant. Electron. Moscow* **15**, 1106 (1988) [*Sov. J. Quantum Electron.* **18**, 710 (1988)].
- [5] L. I. Schiff, *Phys. Rev.* **132**, 2194 (1963).
- [6] P. Sandars, *Phys. Rev. Lett.* **19**, 1396 (1967).
- [7] See, e.g., E. A. Hinds, *Phys. Scr.* **T70**, 34 (1997).
- [8] O. Sushkov and V. Flambaum, *Zh. Eksp. Teor. Fiz.* **75**, 1208 (1978) [*Sov. Phys. JETP* **48**, 608 (1978)].
- [9] M. Kozlov and T. Titov (private communication); see also M. Kozlov and L. Labzowsky, *J. Phys. B* **28**, 1933 (1995), and Ref. [4]. As discussed in these references, the maximum effective field Q in the $a(1)$ state of PbO is somewhat suppressed compared to the best cases, due to an unfavorable electronic configuration.
- [10] G. Herzberg, *The Spectra and Structures of Simple Free Radicals* (Cornell University Press, Ithaca, 1971).
- [11] S. A. Murthy, D. Krause, Jr., Z. L. Li, and L. R. Hunter, *Phys. Rev. Lett.* **63**, 965 (1989).
- [12] J. P. Jacobs *et al.*, *Phys. Rev. A* **52**, 3521 (1995).

- [13] See, e.g., P. Bucksbaum, E. Commins, and L. Hunter, *Phys. Rev. D* **24**, 1134 (1981); I. Davies, P. Baird, and J. Nicol, *J. Phys. B* **21**, 3857 (1988). In both of these, fields >200 V/cm were achieved in hot metal-vapor cells.
- [14] F. Martin *et al.*, *Spectrochim. Acta A* **44**, 889 (1988).
- [15] G. Herzberg, *Molecular Spectra and Molecular Structure, Vol. I: Spectra of Diatomic Molecules* (Van Nostrand Reinhold, New York, 1950).
- [16] W. Beattie, M. Revelli, and J. Brom, *J. Mol. Spectrosc.* **70**, 163 (1978).
- [17] *CRC Handbook of Chemistry and Physics*, edited by R. Weast (Chemical Rubber Company, Cleveland, 1967).
- [18] K. Huber and G. Herzberg, *Molecular Spectra and Molecular Structure, Vol. IV: Constants of Diatomic Molecules* (Van Nostrand Reinhold, New York, 1979).
- [19] See, e.g., S. Haroche, in *Topics in Applied Physics*, edited by K. Shimoda (Berlin, Springer-Verlag, 1976), Vol. 13, pp. 253–313.
- [20] I. Sobelman, *Atomic Spectra and Radiative Transitions* (Springer-Verlag, New York, 1979).
- [21] D. Budker and D. DeMille (unpublished).
- [22] H. G. Howell, *Proc. R. Soc. London, Ser. A* **153**, 683 (1936); E. E. Vago and R. F. Barrow, *Proc. Phys. Soc. London* **59**, 449 (1947); R. F. Barrow, J. L. Deutsch, and D. N. Travis, *Nature (London)* **191**, 374 (1961).
- [23] R. C. Oldenborg, C. R. Dickson, and R. N. Zare, *J. Mol. Spectrosc.* **58**, 283 (1975).
- [24] E. A. Dorko, J. W. Glessner, C. M. Ritchey, L. L. Rutger, J. J. Pow, L. D. Brasure, J. P. Duray, and S. R. Snyder, *J. Chem. Phys.* **102**, 349 (1986).
- [25] M. G. Kozlov, *Zh. Eksp. Teor. Fiz.* **89** 1933 (1985) [*Sov. Phys. JETP* **62**, 1114 (1986)].